EVALUATING PERFORMANCE OF MAJORITY RULES IN PER-PIXEL AND OBIA LAND-COVER CLASSIFICATION USING WORLDVIEW MULTISPECTRAL IMAGERY OF URBAN FRINGE AREA, INDONESIA

Projo Danoedoro[1], Diwyacitta Dirda Gupita[1,3], Pronika Kricella[2]
[1]Remote Sensing Laboratory, Department of Geographical Information Science, Universitas Gadjah Mada, Bulaksumur Yogyakarta 55281, Indonesia
Email: projo.danoedoro@geo.ugm.ac.id
[2]Remote Sensing MSc Program, Department of Geographical Information Science, Universitas Gadjah Mada, Bulaksumur Yogyakarta 55281, Indonesia,
Email: pronikakricella@mail.ugm.ac.id
[3]Department of Geography, Norwegian University of Science and Technology (NTNU), Moholt Alle 6 - 32, 7050 Trondheim, Norway
Email: diwyacig@stud.ntnu.no

KEY WORDS: OBIA, majority filter, land-cover classification, Worldview, Indonesia.

ABSTRACT: OBIA classification has been considered as being able to overcome the limitations of per-pixel methods for high-spatial resolution images. On the other hand, per-pixel classification also often relies on the use of majority filters to generalize the appearance of various classes that give a salt-and-pepper effect. This study aimed to evaluate the performance of the two classifications with different approaches, *i.e.* simple OBIA and majority filters of the per-pixel classification results, using Worldview multispectral imagery of Salatiga, Indonesia. In this study, each classification method applied a combination of several different parameters to derive land-cover maps. In the OBIA classification, the author used two main steps, namely segmentation and object-based classification. For the segmentation process, several parameters were combined with different values including the weights of input spectral bands, average and variance, moving window size, and similarity tolerance. Hundreds of generated segments were selected in spectral sampling of each land cover class. Based on these samples, per-pixel classification was then run to derive a pixel-based land-cover map. After that, the pixel-based map was processed in two different ways, *i.e.* (a) combined with the segmentation result to generate an object-based land-cover map through majority rule in each segment, and (b) majority-filtered at various window sizes to derive land-cover maps with different levels of generalization. Independent field data was used for accuracy assessment of the maps. We evaluated the accordance between maps by superimposing the OBIA-based with the majority-filtered maps. It was found that the combination of different parameters resulted varying accuracies of OBIA classification, and likewise with the accuracies of the majority-filtered results. We also found that the accordance between the OBIA classification results and the classified images varied with the window size, where the 7x7 filter gave the highest match between the OBIA and the filtered per-pixel classification, *i.e.* 80.29%.

1. INTRODUCTION

1.1 Background and Objective

Image classification is still one of the most important activities in remote sensing, because it can derive thematic information needed in various geographic analyses (Giri, 2012; Danoedoro, 2019). For high-spatial resolution images (5 m or higher), the use of per-pixel classification is considered inadequate, because the pixel size is much higher than the size of the object being classified (Baatz and Schappe, 2000). Object-based classification, which is included in OBIA (Object-based Image Analysis), is considered capable of overcoming the limitations of per-pixel classification because it is able to classify object features as a collection of pixels contextually by taking into account various textural parameters (color, shape, size, texture, pattern) and even being able to accommodate landscape metrics considerations (Jensen, 2015; Lebourgeois *et al*., 2017; Ventura *et al*., 2018; De Castro *et al*., 2018).

There are many object-based classification methods, but in the last two decades this classification method mostly accommodates object-based segmentation methods first (Dragut *et al*., 2014; Blaschke *et al*., 2016; Eastman, 2019), to divide all pixels in the study area into segments or polygons, each of which represents the appearance of a particular object. The second step in classification is to take samples in the form of a spectral signatures based on representative segments to become regions of interest (ROIs) without drawing polygon lines but using polygon boundaries in the form of existing segments. Spectral signature of each sample segment which represents the type

or class of objects were then extrapolated as an identifier to label the classes of other segments in the image.
The decision to classify all these segments is substantially different from one algorithm to another (Elhadi and Zomrawi, 2009; Hussein, 2013; Blaschke *et al*., 2014; Ventura *et al*., 2018). The simplest method used by Eastman (2019) includes the following steps: (a) using the segment spectral signature as input in the per-pixel classification and generating a per-pixel classified image, (b) combining the per-pixel classified image with the segmented image to derive the majority class that appears most often in each segment, and replaces the segment label with reference to the class that occurs most often. In other words, object-based classification as developed by Eastman (2019) is a method of aggregating the results of segment-based classification, and gives a generalization effect at the segment level. The result of this process is a land-cover/land-use map in both a raster and vector data models, which can be edited in a vector-based GIS environment (Danoedoro, 2020).

On the other hand, the nominal filtering method in the form of a majority filter has also been commonly used as an effort to generalize the direct results of per-pixel multispectral classification, in order to reduce the salt-and-pepper effect (Gao, 2010; Mather and Koch, 2011; Ma and Nie, 2018). The results of the multispectral classification contain land cover class labels filtered by the convolution method through moving windows measuring 3x3, 5x5, 7x7 and so on, and in each window a majority label (mode) is determined which replaces the label in the center of the window. The larger the filter window size, the more generalized the appearance of the classification results. This method is able to produce classified and generalized images that have the potential to be converted into vector data models through raster-to-vector conversion, for later editing in a vector-based GIS environment (Danoedoro, 2019).

The availability of these two methods for deriving vectorized raster maps resulting from a certain level of generalization raised curiosity regarding the effectiveness of the methods and the resultant accuracy, particularly when they were applied to images with different levels of generalization. Based on this background, this study aimed to compare the effect of the use of the majority rules on the results of object-based classification and majority filtering and relate them to the accuracy obtained.

1.2 Study area and Materials

This study made use Worldview-2 imagery covering the urban fringe area of Salatiga, Central Java, Indonesia with 2000 x 2000 pixels and at 2 m spatial resolution, which means represents an area of 4 x 4 km^2. The image was recorded on 18 May 2018 and available in eight spectral bands (coastal, 400 - 450 nm; blue, 450 - 510 nm; green, 510 - 580 nm; yellow, 585 - 625 nm; red, 630 - 690 nm; red edge, 705 - 745 nm; near infrared-1, 770 - 895 nm; and near infrared-2, 860 - 1040 nm). We did not utilize the shortwave infrared bands due to their different spatial resolution. An overview of the study area is given in Figure 1, which is presented in standard false color composite image. As showed in Figure 1, the study area consists of various land-cover/land-use categories such as settlement and other urban buildings, agricultural land with annual crops including rice, mixed garden, rubber plantation, and a small portion of natural lake partly covered with aquatic weed (*Eichhornia crassipes*).

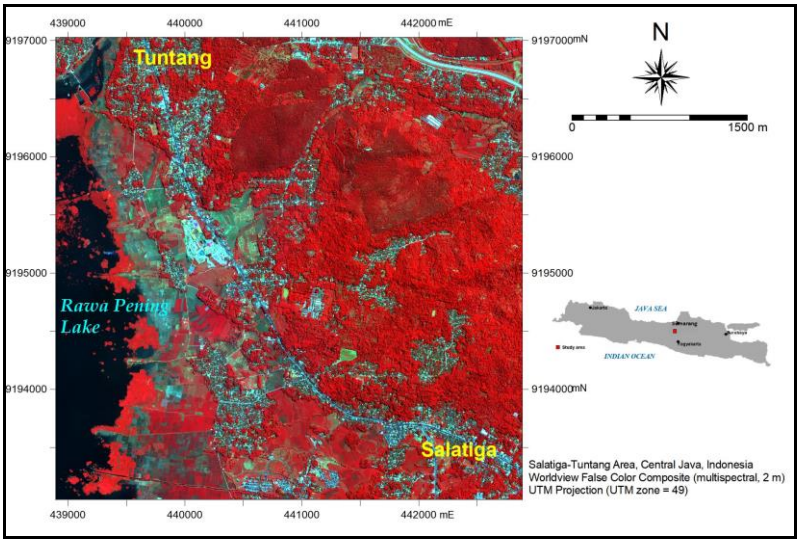

Figure 1. Study area as represented by a false color composite Worldview imagery

2. METHODS

The author developed methods in this study and organized them into three stages. The first was object-based image segmentation, followed by per-pixel classification and majority filtering-based generalization. The second was object-based classification using segmentation and per-pixel classification results. While the third was accuracy assessment of resultant maps, followed by map-to-map comparison involving the OBIA and majority-filtered classification results in various window sizes. Figure 2 depicts the procedure developed in this study.

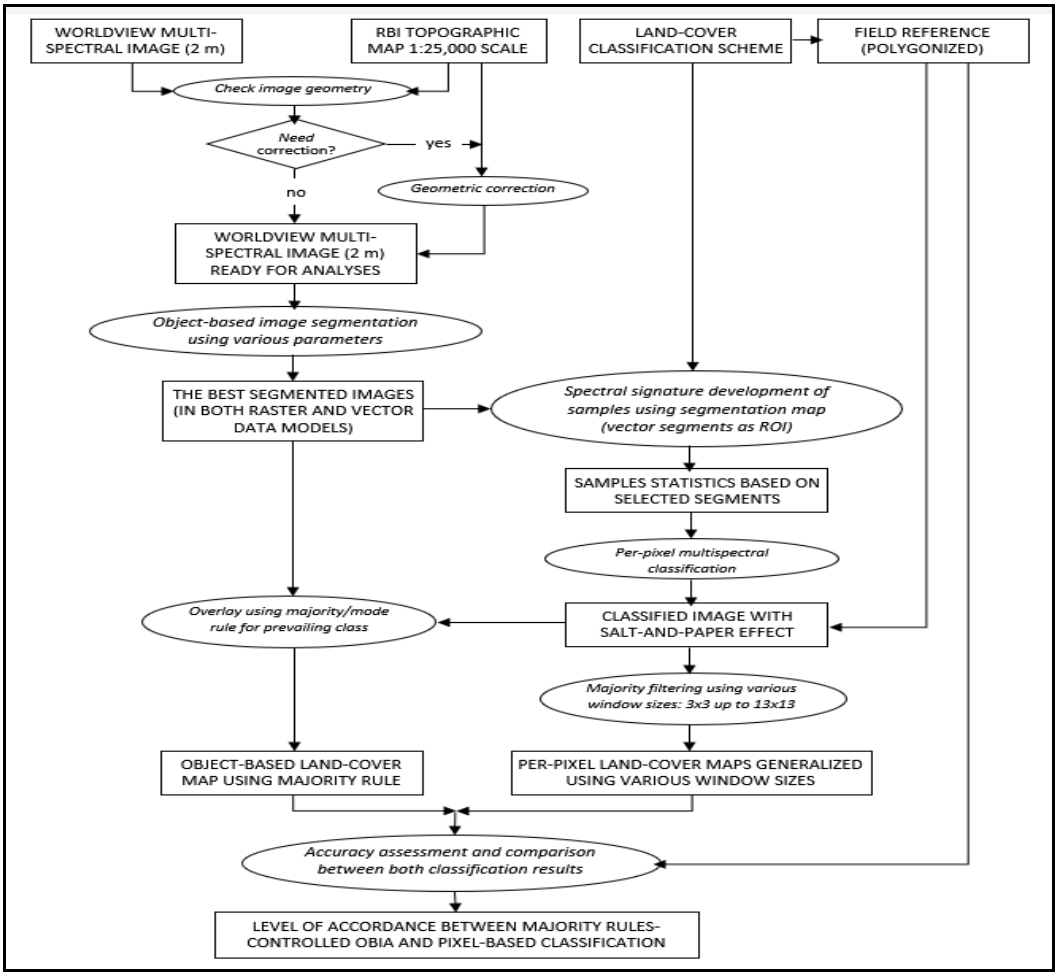

Figure 2. Flow diagram of the study

2.1 Per-pixel Classification and Majority Filtering

Per-pixel classification worked using supervised approach, where the samples were taken based on the prior knowledge of the land-cover in the study area. The prior knowledge was supported by field orientation, local knowledge, and conceptual understanding about the relationship between land-cover and spectral response. In order to make a fair comparison, the per-pixel classification also made use of the same samples (segment-based ROIs) utilized by the object-based classification (see Figure 2 and explanation in sub section 2.2). This study applied four per-pixel classification algorithms, *i.e*. minimum distance to mean, K-nearest neighbor, maximum likelihood, and support vector machine (SVM) (Mather and Koch, 2011; Mountrakis *et al*., 2011; Eastman, 2019). After that, we carried out accuracy assessment on each classification result using independent field reference. The validating field reference were in form of polygons, collected during field observation. We selected the validating samples using a computer-based stratified random sampling approach, although we also made some adjustment due to the circumstances in the field, particularly in the swampy area. Following the per-pixel classification, this study also applied a set of majority filters to the original resultant land-cover maps. We used 3x3, 5x5, 7x7, 9x9, 11x11 and 13x13 window size filter to generalize the classified pixels.

2.2 Image Segmentation and Object-based Classification

This study made use of OBIA classification with respect to the one developed by Egberth and Nilsson (2010) and Eastman (2019). The OBIA classification consisted of several stages, *i.e.* (a) object-based image segmentation, (b) spectral signature development using several resultant segments as region of interest (ROI)-based samples, (c) per-pixel classification using the ROI or segment-based samples, and (d) object-based classification by combining the segmentation results and the per-pixel classification image.

The segmentation process followed a watershed definition-like procedure, which can be categorized as edge detection segmentation (Egberth and Nilsson, 2010; Gonzales and Woods, 2017; Johnson and Lei, 2020; Badhori *et al*., 2020.), where the image pixels were divided into small regions according to their variance. The low variance within a given moving window indicates a relatively homogeneous objects, while the high variance indicates boundary between two regions. This method worked iteratively, controlled by a set of parameters including window size, input spectral band weights, variance weights, mean weights, and similarity tolerance. Low similarity tolerance would let the adjoining defined regions with certain statistical characteristics remain separated, while high similarity tolerance made several regions with similar statistical characteristics joined together into larger ones.

Once the segmented image delivered, a process of evaluation was carried out by overlaying the segment map (in vector model) on the color composite images. Several color composite images (true color, standard false color, and PCA-based false color) were required to ensure that the segments matched with the land-cover boundaries perceived, with respect to the land-cover classification scheme used in this project. This study utilized a classification scheme developed by Danoedoro (2019), which differentiates land-cover/land-use dimensions into spectral, spatial, temporal, ecological and socio-economic aspects. Based on the evaluation, other combinations of segmentation parameters were run to generate the best segmented maps.

The segmented map was then used as a basis for spectral signature development. The authors selected segments as ROI, and the spectral signature of pixels within each segment was computed. The spectral signature files were then used in a per-pixel classification to derive a pixel-based land-cover map. The object-based image classification was carried out by overlaying the resultant pixel-based land-cover map (which performs salt-and-pepper effect) with the segmented image (in raster data model). A majority rule converted the per-pixel land-cover map into object-based one by taking the predominant class or label existing in each segment as the prevailing land-cover class.

2.3 Classification Comparison

Comparison between OBIA and per-pixel classification results worked by overlaying several pairs of OBIA and original classification results, as well as majority-filtered land-cover maps. By overlaying these maps, the accordance between them could be obtained and analyzed in relation with the accuracy achieved. The comparison results were presented in terms of tables and maps.

3. RESULTS AND DISCUSSION

3.1. Per-pixel Classification and Majority Filtering Results

This study made use of the per-pixel classification result, which was classified using spectral signature samples from the segment-based ROIs. We tested four classification algorithms, *i.e.* minimum distance to mean, K-nearest neighbor, maximum likelihood, and SVM. All algorithms used the same spectral signature samples. As shown in Table 1, the maximum likelihood algorithm could achieve the best overall accuracy, *i.e.* 74/86 %, although it was much lower as compared with the one achieved by the best OBIA classification result that achieved 88.61 %.

Table 1. Per-pixel classification accuracy using various algorithms.

Per-pixel Classification Algorithm	Accuracies achieved (%)		
	Average Accuracy	Average Reliability	Overall Accuracy
Minimum distance to mean	60.66	58.98	70.34
K-nearest neighbor	62.05	59.74	73.02
Maximum likelihood	62.47	60.43	74.86
Support vector machine	62.76	60.21	73.45

Note: Average accuracy = average producer's accuracy, average reliability = average user's accuracy

Based on the obtained per-pixel classification results, we applied majority filtering to the best one, *i.e*. the maximum likelihood-based land-cover map, using 3x3 up to 13x13 window sizes. Each majority filtered land-cover map was then superimposed with the same independent field dataset containing polygons, which has been utilized for accuracy assessment of OBIA-based and pixel-based land-cover maps. This study found that the best majority-filtered land-cover maps --as viewed from their accuracy-- were the ones filtered using 7x7 window size. This means that majority filtering technique could improve the quality of per-pixel classification result, particularly at 7x7 window size. This finding confirmed the results obtained by previous studies (Danoedoro 2006; Danoedoro, 2009), which used Landsat ETM+ and Quickbird imagery. Figure 3 shows the comparison between original and majority-filtered classification results. The majority filter reached the highest accuracy at 7x7 window size, *i.e.* 84.53%. and this peak gradually decreases when the window size increases to 9x9, 11x11, and 13x13 respectively.

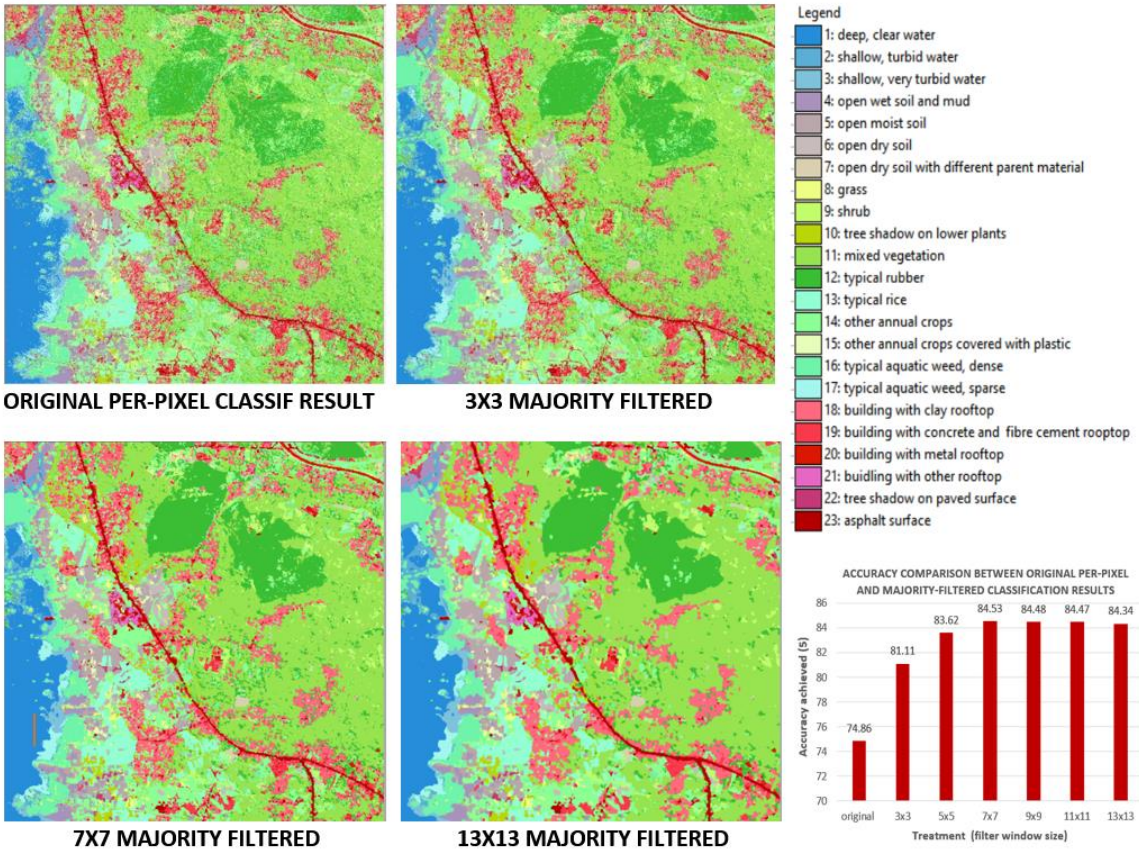

Figure 3. Original per-pixel classification result and examples of majority-filtered ones. Graphics on the bottom right corner shows the complete results.

3.2. Segmentation Results

This study tried 13 combinations of parameters for carrying out the segmentation process. The first 10 combinations focused on the weight of the input bands. The default was evenly distributed weights for each band. After that, the more weights were given to near infrared and red bands, and then PCA bands which were less correlated with others. Further modification was applied to the variance and mean weights, by which the increase of one parameter automatically reduced the other one, since the total weight is 1.0. Finally, changes were given to the value of similarity tolerance, where the smaller value indicates more detailed segments. Evaluation of the segmentation results were carried out by overlaying the segments in vector data model on the color composite images (Figure 4).

Table 2. Parameters used for the best three object-based segmentation and classification and their accuracies

Segmentation Version	Window Size	Input band weights										Mean&Var Weight		Similrty Tolerance	Accuracy (%)		
		Band 1	Band 2	Band 3	Band 4	Band 5	Band 6	Band 7	Band 8	PC 1	PC 2	Mean	Var		Overall	Avg Accu	Avg Reliab
1	3x3	0.117	0.117	0.117	0.117	0.15	0.117	0.15	0.117	-	-	0.5	0.5	20	82.21	70.15	71.00
2	3x3	0.10	0.10	0.10	0.10	0.10	0.10	0.10	0.10	0.10	0.10	0.4	0.6	15	84.02	71.17	71.82
3	3x3	0.075	0.075	0.075	0.075	0.075	0.075	0.075	0.075	0.30	0.10	0.4	0.6	20	88.61	78.47	82.91

3.3. OBIA Classification Results

Based on a total of 360 samples using existing segments as ROIs, per-pixel classification was run to generate the pixel-based land-cover map. In the object-based classification, the pixel-based land-cover map was then super-imposed with the segment map previously produced (see Figure 4). The OBIA classification procedure applied a majority or mode rule to take the predominant class within each segment, so that the object-based land-cover map could be delivered. A total of three versions of object-based land-cover map have been produced and further considered in the next analysis, generated from the highest accuracies they achieved among others. Two combinations made use of PC1 and PC2 images generated using principal component analysis of the eight original bands, and they achieved the best accuracy levels. Accuracy assessment of these OBIA products was carried out by using 291 samples of polygons (containing 106,367 pixels), taken independently in the field with the support from pan-sharpened Worldview and Google Earth imagery. These polygons were then superimposed with the produced OBIA maps in order to generate error matrices of accuracy assessment according to Congalton and Green (2019). Table 2 depicts the three OBIA land-cover maps with the highest accuracies have different combination of segmentation parameters, while Figure 5 shows them visually.

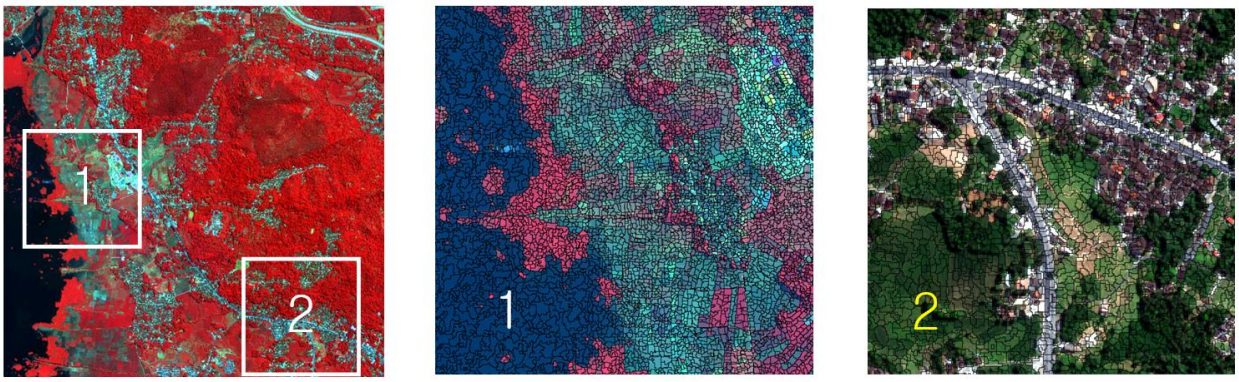

Figure 4. The entire coverage of the study area and two examples (one in false color and the other one in true color) of small portion that have been segmented. © Worldview image copyright DigitalGlobe (2018).

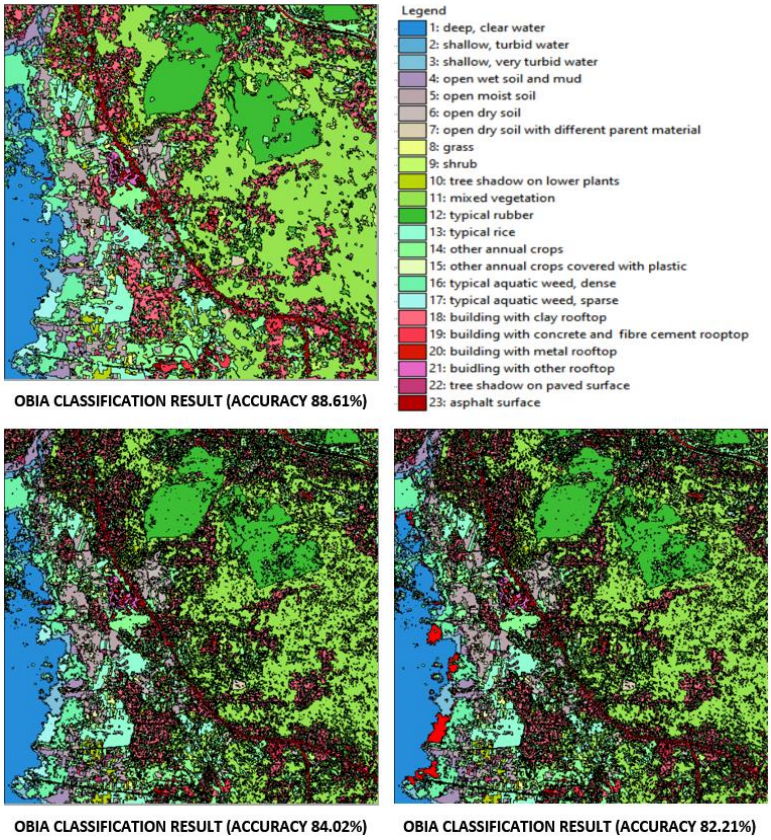

Figure 5. Three examples of OBIA land-cover classification result at different accuracies.

3.4. Comparison between OBIA and Pixel-pixel Classification Results

In order to make a fair comparison between the OBIA and the per-pixel classification results, this study tried to control other variables in such a way so that they were kept the same. The spectral signature of samples for the OBIA and the per-pixel classifications were exactly the same. The per-pixel classification result used as input to the object-based classification was also the same as the one that majority filtered. Furthermore, the independent dataset for accuracy assessment, which contain polygons, were the same in location, number of polygons and pixels, as well as the number of classes.

Prior to spatial comparison between two classification approaches, we compared the results statistically. The per-pixel classification produced land-cover maps with relatively low overall accuracy, even using the best algorithm and support vector machine, which only reached 74.86% and 73.45% respectively. Similar results have been obtained by Sibaruddin *et al.* (2018) and Putri and Danoedoro (2019) using two different classification schemes. These values where much lower than those of the best three OBIA classification results. The use of majority filtering could increase the accuracy, and this reached the peak in around 5x5 up to 9x9 filter window size, which confirmed previous results by Daneodoro (2006) and Cui *et al*. (2018), even though the best accuracies achieved were still lower than those of OBIA classification results.

Figure 6 shows a map-to-map comparison method for evaluating the level of accordance or match rate between the OBIA and per-pixel classification results. A simple Boolean logic was run in order to classify the results into "match" and "not match". We defined "match" class when the superimposed maps found that pixels on the same coordinates exhibit the same class, and "not match" was defined when they were otherwise. Figure 7 shows different results when three versions of OBIA classification result were superimposed with the original and majority-filtered per-pixel land-cover maps. There were three version of OBIA land-cover maps generated using different combination of parameters, which achieved relative high accuracy. The first one has 82.21% accuracy, the second one reached 84.02%, and the last one achieved the best accuracy, *i.e.* 88.61%.

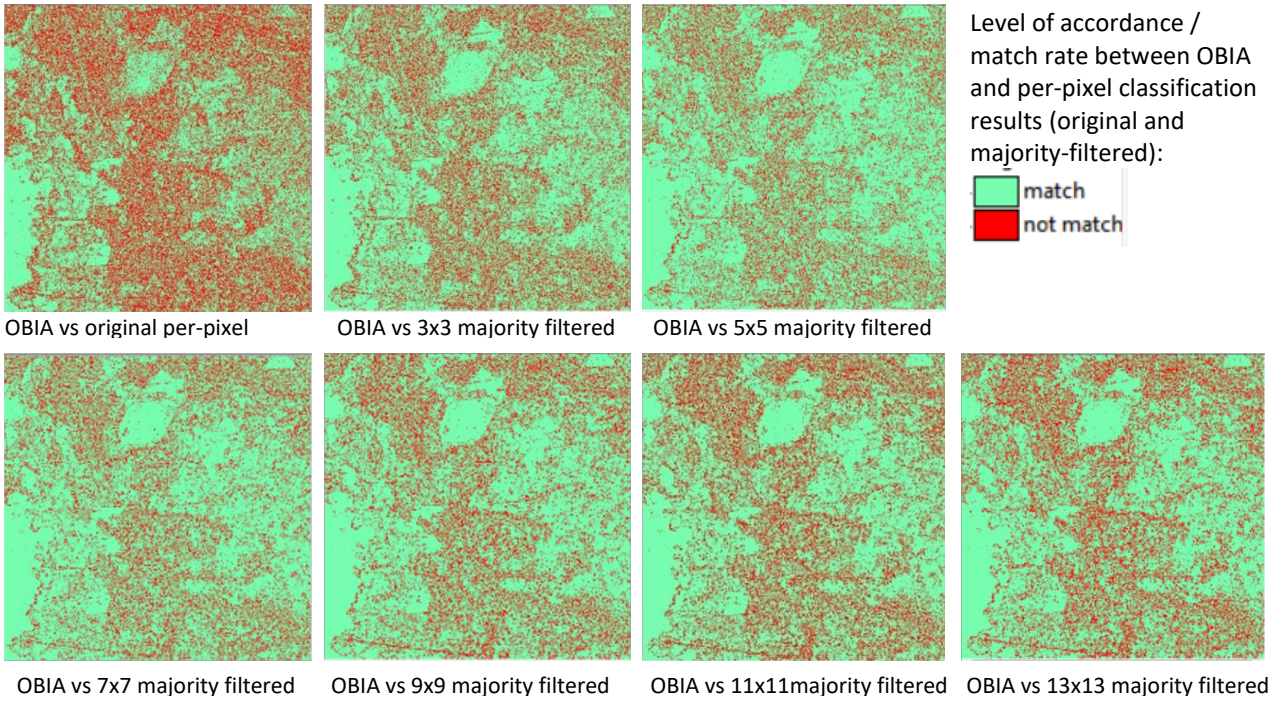

Figure 6. Accordance levels between the OBIA classification at 88.61% accuracy and the per-pixel land-cover maps

Figure 7 shows the pattern of changes in the match level of the majority filtered- and the OBIA classification results (in the form of a bar chart), which is compared to the pattern of changes in the accuracy of each map of the majority filtered per-pixel classification. We performed this analysis for the three results of the OBIA classification separately, and each has a different accuracy level.

In Figure 7a, with an OBIA classification accuracy of 82.21%, it can be seen that the trend of the match rate between the majority filtering and OBIA results increased until the filter window size is 5x5 (77.15%), and then continued to decrease until the window size is 13x13. This pattern was not in line with the one of increasing accuracy of the majority filtering results, where the highest accuracy (84.53%) was achieved at a 7x7 window size. In the Figure 7b with an OBIA classification accuracy of 84.02%, the highest match between the OBIA results and the majority filtering was achieved at the 5x5 filter window size (80.26%), although with a very small difference as compared to the 7x7 filter window size with a match rate of 79.93%. The highest accuracy of the filtering results as a comparison was the same, *i.e.* 84.53% at the 7x7 filter window size. In the Figure 7c, with the accuracy of the OBIA classification results of 88.61%, the trend of the two models was almost the same, where the accordance between the two models reaches the peak of the 7x7 filter window size with a match level of 80.29%.

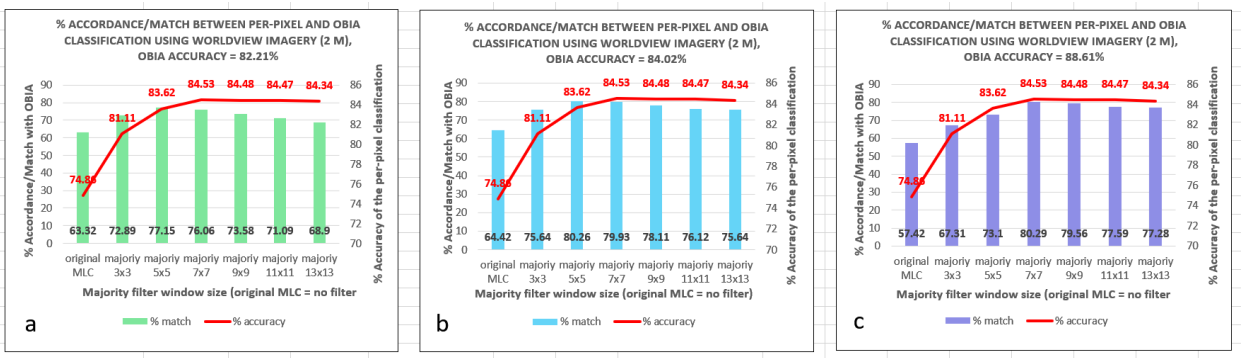

Figure 7. Accordance between OBIA and per-pixel classification results, as compared to the accuracies achieved.

One thing that distinguishes the three figures was the level of similarity between the filtering results' trend of accuracy and the trend of the accordance between the two models. In the Figure 7a, where the accuracy of the OBIA classification results was lowest, the pattern was the most different; while in the Figure 7c, which used the

results of the OBIA classification with the highest accuracy, the patterns were the most similar. That is to say, the level of accordance between the two models was influenced by the level of accuracy of each approach.

Since this observation was only carried out using a single spatial resolution, *i.e.* 2 m with Worldview imagery, more general conclusion can only be made when several images with different spatial resolutions are involved. Therefore, this study also recommend the use of other images with various spatial resolutions to be observed.

4. CONCLUSIONS

In a land-cover mapping based on digital classification of resolution imagery such as Worldview, a simple OBIA classification using majority rule was able to provide higher accuracy than multispectral classification with a per-pixel approach. However, the per-pixel classification accuracy could increase when a majority filtering applied. The accuracy increased at 7x7 filter window size, and then decreased until the window size reached 13x13, even though the highest accuracy achieved was still lower than that of OBIA. Based on the comparison between the majority rules applied to OBIA and per-pixel classifications, this study found that the accordance between the two approaches tended to be higher when the two maps being compared also have high accuracies.

ACKNOWLEDGEMENT

The authors wish to thank the Digital Globe for delivering the Worldview imagery under the Digital Globe Foundation Program in collaboration with Faculty of Geography, Universitas Gadjah Mada, 2018. Funding support from the Faculty of Geography, Universitas Gadjah Mada is also acknowledged.

REFERENCES

Baatz, M. and Schäpe, A., 2000. Multiresolution segmentation: an optimization approach for high quality multiscale image segmentation. Angewandte Geographische Informationsverarbeitung XII, pp. 12–23.

Bhadoria, P., Agrawal, S., Pandey, R., 2020. Image Segmentation Techniques for Remote Sensing Satellite Images. IOP Conference Series: Materials Science and Engineering 993 (2020) 012050. IOP Publishing, doi:10.1088/1757-899X/993/1/012050

Blaschke, T., Hay., G.J., Kelly, M., Lang, S., Hofmann, P., Addink, E., Feitosa, R.Q., van der Meer, F., van der Werff, H., van Coillie, F., and Tiede, C., 2014, Geographic Object-Based Image Analysis – Towards a new paradigm, ISPRS Journal of Photogrammetry and Remote Sensing (87) pp. 180–191

Blaschke, T., Kelly, M., and Merschdorf , H., 2016. Object-Based Image Analysis: Evolution, History, State of the Art, and Future Vision. In: Thenkabail, P.S. (ed.) Remote Sensing Handbook Volume I -- Remotely Sensed Data Characterization, Classification, and Accuracies. CRC Press, Boca Raton.

Congalton, R. G., and Green, K., 2019, Assessing the Accuracy of Remotely Sensed Data - Principles and Practices, Third Edition. John Wiley & Sons, New York

Cui, G., Lv, Z., Li, G., Benediktsson, J. A., and Lu, Y., 2018, Refining Land Cover Classification Maps Based on Dual-Adaptive Majority Voting Strategy for Very High Resolution Remote Sensing Images. Remote Sensing, (10), pp. 1238-1257. doi: 10.3390/rs10081238

Danoedoro, P., 2006, Extracting Land-use Information Related to Socio-economic Function from Quickbird Imagery: A Case Study of Semarang Area, Indonesia, Proceedings of the Map Asia 2006 “GeoICT for Good Governance”, Bangkok.

Danoedoro, P., 2009, Land-use information from the satellite imagery: Versatility and Contents for Local Physical Planning, Academic Publishing, Saarbrucken.

Danoedoro, P., 2019. Multidimensional Land-use Information for Local Planning and Land Resources Assessment in Indonesia: Classification Scheme for Information Extraction from High-Spatial Resolution Imagery. Indonesian Journal of Geography, (51) 2, pp. 131-146.

Danoedoro, P., 2020. Pengaruh Tingkat Kompresi Citra ALOS AVNIR-2 terhadap Akurasi Hasil Transformasi

Indeks Vegetasi dan Klasifikasi Penutup Lahan Wilayah Salatiga dan Ambarawa, Jawa Tengah. Majalah Geografi Indonesia (34), 2, pp.130 – 139

De Castro, A.I., Torres-Sánchez, J., Peña, J.M., Jiménez-Brenes., F.M., Ovidiu Csillik, and López-Granados, F., 2018, An Automatic Random Forest-OBIA Algorithm for Early Weed Mapping between and within Crop Rows Using UAV Imagery. Remote Sens. 2018, (10) 2, pp. 285-305. doi: 10.3390/rs10020285

Dragut, L., Csililik, O., Eisank, C., and Tiede, D., 2014, Automated Parameterisation for Multi-Scale Image Segmentation on Multiple Layers. ISPRS Journal of Photogrammetry and Remote Sensing, (88), pp. 119-127. doi: 10.1016/j.isprsjprs.2013.11.018

Eastman, J.R., 2019. Idrisi TerrSet – Guide to GIS and Image Processing, Clark Labs, Clark University, MA: Worchester.

Egberth, M. and Nilsson, M., 2010. KNN-Sweden--Current map data on Swedish Forests. In: Proceedings ForestSat 2010: Operational Tools in Forestry using Remote Sensing Techniques, September2010, pp. 265-267.

Elhadi E.M., and Zomrawi, N. 2009. Object-based Land use/cover Extraction from QuickBird image using Decision tree. Nature and Science, (7), 10, pp. 1-12

Gao, J., 2010, Digital Analysis of Remotely Sensed Imagery. McGraw Hill, New York

Giri, C. P. (ed), 2012. Remote Sensing of Land Use and Land Cover - Principles and Applications. CRC Press, Boca Raton

Gonzales, R.C., and Woods, R.E., 2017. Digital Image Processing, 4th edition. Pearson, New York.

Hussein, S., 2013. Object Based Image Analysis (OBIA) for Land Cover Mapping in a Heterogeneous Landscape: A Comparison of Sample Based and Rule Based Classification. Proceedings of the 34th Asian Conference on Remote Sensing (ACRS). Bali, Indonesia.

Jensen, J. R., 2015. Introductory Digital Image Processing – A Remote Sensing Perspective, 4th edition. Prentice Hall, Englewood Cliffs, N.J.

Johnson, B. A., and Ma, L, 2020. Image Segmentation and Object-Based Image Analysis for Environmental Monitoring: Recent Areas of Interest, Researchers' Views on the Future Priorities. Remote Sensing, (12), pp. 1772-1780. doi:10.3390/rs12111772

Lebourgeois, V., Dupuy, S., Vintrou, E., Ameline, M., Butler, S., and Bégué, A., 2017. Combined Random Forest and OBIA Classification Scheme for Mapping Smallholder Agriculture at Different Nomenclature Levels Using Multisource Data (Simulated Sentinel-2 Time Series, VHRS and DEM). Remote Sensing. (9), 3, pp. 259-278. doi: 10.3390/rs9030259

Ma, H., and Nie, Y., 2018. A two-stage filter for removing salt-and-pepper noise using noise detector based on characteristic difference parameter and adaptive directional mean filter. PLOS ONE. doi: 10.1371/journal.pone.0205736

Mather, P.M., and Koch, M., 2011. Computer Processing of Remotely-Sensed Images: An Introduction, 4th Edition. John Wiley and Sons, London.

Mountrakis, G., Im, J., and Ogole, C., 2011. Support vector machines in remote sensing: A review, ISPRS Journal of Photogrammetry and Remote Sensing (66) 3, pp. 247-259.

Putri, E. A. W., and Danoedoro, P., 2019. "Comparing per-pixel and object-based classification results using two different land-cover/land-use classification schemes: a case study using Landsat-8 OLI imagery," Proc. SPIE 11372, Sixth International Symposium on LAPAN-IPB Satellite, 1137206 (24 December 2019); doi: 10.1117/12.2541876

Sibaruddin,H. I., Shafri, H.Z.M., Pradhan, B., and Haron, N.A., Comparison of pixel-based and object-based image classification techniques in extracting information from UAV imagery data, IOP Conference Series: Earth and Environmental Science 169 (2018) 012098. doi : 10.1088/1755-1315/169/1/012098

Ventura, D., Bonifazi, A., Gravina, M. F., Belluscio, A. and Ardizzone, G., 2018. Mapping and Classification of Ecologically Sensitive Marine Habitats Using Unmanned Aerial Vehicle (UAV) Imagery and Object-Based Image Analysis (OBIA). Remote Sensing, (10) 9, pp. 1331- 1353. doi : 10.3390/rs10091331